Numerical investigation of the behavior of the church of Agia Triada, Drakotrypa, Greece

G. C. Manos, V. J. Soulis & A. Diagouma
Department of Civil Engineering, Aristotle University of Thessaloniki, Greece

Abstract

This paper includes the most important findings of a series of linear analyses focusing on the development of failure that is identified through different failure criteria. The historic monument which was selected for this investigation is the church of Agia Triada, in the District of Karditsa, Greece. The numerical simulation for the church of Agia Triada includes all parts of the super-structure and considers the effects of vertical and earthquake loads. The main objective of this paper is to predict the initiation of failure at various structural elements considering a) a Mohr-Coulomb failure criterion with a limit on tension strength and b) modified Von Misses failure criterion. These two failure criteria are applied for the same structure and for the same load combinations. The predicted by the two failure criteria initiation of failure and the corresponding failure areas are compared and discussed.
Keywords: historic monuments, numerical investigation, Mohr-Coulomb, modified Von Misses.

1 Introduction

Masonry is a material that presents considerable difficulty in assigning values of mechanical properties or adopting failure criteria. Different simulation strategies can be applied depending on the scale needed for the examination of the initiation of failure in the masonry. Micro-modeling of the masonry, where units and mortar joints are simulated separately, together with appropriate failure criteria is a popular approach in successfully predicting failure areas in masonry components. However, it is very computationally demanding to be directly applied in large structures, especially those with considerably complicated formations like monumental structures. An alternative approach for such structures is macro-modeling where the masonry is considered as an anisotropic composite. This type of modeling is combined with failure criteria that are applied to this anisotropic medium.

Apart from modeling the complex architectural features, some of the main difficulties in numerical simulation approximations are also the following ([1], [2], [3]):

- Understanding the importance of the load transfer mechanisms, for both the gravitational and seismic forces. In this way certain simplifications can be introduced in representing the structural system by the numerical model.
- Employing linear or non-linear numerical approximations combined with the difficulty in assigning values to important physical properties.

The current numerical study includes linear dynamic analyses for the determination of the fundamental eigen-modes and frequencies of the Agia Triada Church. Gravitational and earthquake loads were applied in order to identify certain areas of the load-bearing system that exhibit stress concentration that reaches critical tensile compressive and shear strength values for the stone masonry. Certain failure criteria are then applied in order to identify the failure areas.

2 Numerical analysis of Agia Triada at the prefecture of Karditsa

In this section the numerical study of the behaviour of the church of the Agia Triada of the village of Drakotrypa of the prefecture of Karditsa in Greece will be presented. This church dates from the 1742 A.D. and is a single-nave basilica with a central dome and a transverse nave together with 3 apses at the sides of the church. This church belongs to the post-Byzantine type of construction. The most visible signs of damage are: a) Formation of cracks at the keys of the vaults and arches, b) East-West cracks of the vaulting system parallel to the longitudinal axis of the church.

The material properties adopted in this analysis are determined using the formulas recommended by several references [4] and they are as follows: 1) Young's Modulus = 650fm'; 2) Poisson's ratio 0.2; 3) tensile strength of masonry =0.05fm'; 4) plastic strain at masonry compression failure ranges between 0.0008 and 0.0013.

Table 1 lists values, which were assumed to be valid for the critical mechanical properties for the masonry segments as the current examination did not include any experimental investigation, either at the laboratory or in-situ, for determining such properties.

Table 1: Assumed mechanical characteristics of the stone masonry.

Young's Modulus (N/mm^2)	Poisson's Ratio	Stone Masonry Compressive Strength (N/mm^2)	Stone Masonry Tensile Strength (N/mm^2)
2500	0.2	3.846	0.192

It is recognized by the authors that verification of the values listed in table 1 is highly desirable as the approximation of the results and conclusions of the present study is linked with these assumed values. Such verification can be provided by in-situ and laboratory experimental means. This has been proposed but has not been possible so far due to lack of sufficient resources.
Base fixity was assumed at the foundation level, 600mm below ground level. The numerical study included the determination of the fundamental eigen-modes and frequencies.

The numerical simulation that was adopted utilized thick beam elements and three-dimensional shell elements that are provided in the LUSAS 13.4 software package. Two types of load combinations were examined. The first included **1.35G + 1.5Q** and the second **G + 0.3Q+/-E** where **G** the permanent load, **Q** the snow and live load and **E** the earthquake load. The value for the live load (**Q**) was assumed to be zero. The dead load for the limestone was assumed 24.5KNt/m^3. The roof weight was assumed to be equal to 1.55KN/m^2.

2.1 Mohr-Coulomb failure criterion with tension cut off

The failure surface that was assumed to be valid is schematically presented in figure 1. Failure is introduced when: a) stresses exceed the allowable compressive strength, 3.846 Nt/mm^2 b) stresses exceed the allowable tensile strength of Masonry, 0.192 Nt/mm^2 c) stresses exceed the shear strength of stone masonry. Following the proposed revisions to Eurocode-6 Nov 2002 [5] the shear failure criterion that was adopted is:

$$f_{vk} = f_{vko} + 0.4\,\sigma_n \tag{1}$$

where: f_{vko} is the shear stress of the stone masonry when the normal stress is zero; f_{vko} was assumed to be equal to 0.192 Nt/mm^2. σ_n ís the normal stress

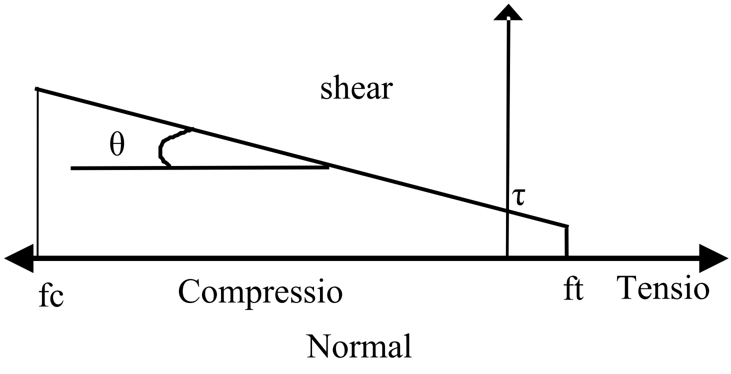

Figure 1: Assumed failure surface used to predict failure of Ag. Triada church structural members.

2.2 Biaxial strength envelope: modified Von-Misses failure criterion

The applicability of an alternative failure criterion has been also investigated, namely the modified Von-Misses failure criterion. The applicability of this failure criterion to masonry was shown by Page [6], who carried out experiments on solid clay masonry subjected to proportional biaxial loading and obtained a failure envelope. This modified criterion differs from the actual Von-Misses criterion in the sense that can predict different behaviour in tension and compression. This modified Von-Misses criterion was checked in a simple numerical experiment before being applied to the church of Agia Triada. This numerical experiment utilized a rectangular wall subjected to biaxial state of stress with masonry mechanical properties the same as the ones used in the simulation of the Agia Triada church. In figure 2a, this masonry wall is presented with its boundary conditions and loading arrangement. In figure 2b, the resulting failure envelope in terms of proportional principal stresses as produced by the application of the modified Von-Misses criterion is shown.

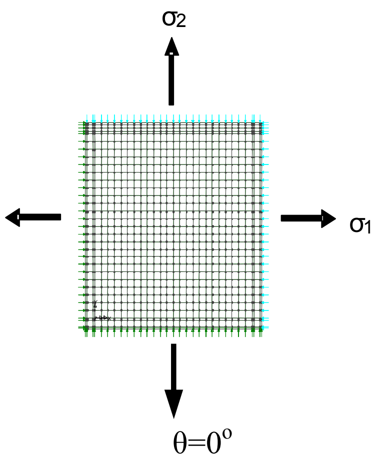

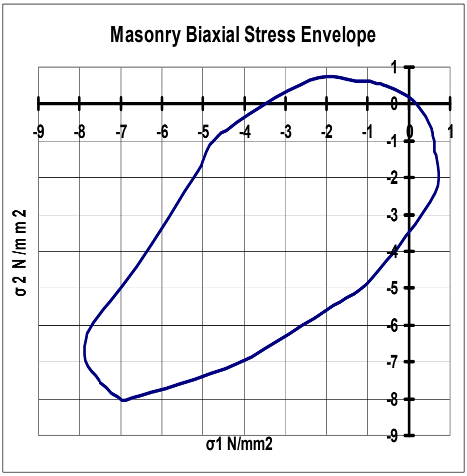

Figure 2: a) Numerical simulation of masonry wall with loading b) Failure envelope obtained in terms of proportional biaxial principal stresses

2.3 Study of the eigen-modes: gravitational and earthquake load behaviour

The numerical study included the determination of the fundamental eigen-modes and frequencies for 6 different numerical simulations in order to determine the contribution of common structural elements (tympana, apses, openings, and secondary vaulting) to the dynamic behaviour of this church (Table 2). The contribution of tympana, apses and openings has been extensively studied in previous works [3]. The main objective of the present study is to predict the contribution of secondary vaulting in the dynamic characteristics of this monument.

Table 2: Modal eigen-periods and mass participating ratios for 6 numerical simulations.

Model 1 without apses and without tympanum	Transverse translational mode T= 0.123 seconds			Longitudinal translational mode T= 0.099 seconds		
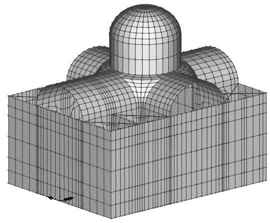	Individual Modal Participating Ratio %			Individual Modal Participating Ratio %		
	Ux	Uy	Uz	Ux	Uy	Uz
	0.00	**52.56**	0.00	**51.21**	0.0	0.006

Model 2 without apses and with tympana	Transverse translational mode T= 0.113 seconds			Longitudinal translational mode T= 0.092 seconds		
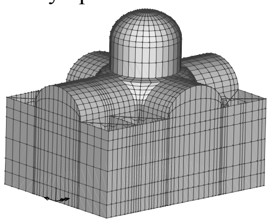	Individual Modal Participating Ratio %			Individual Modal Participating Ratio %		
	Ux	Uy	Uz	Ux	Uy	Uz
	0.00	**58.24**	0.00	**46.60**	0.0	0.022

Model 3 with 1 apse without tympana	Transverse translational mode T= 0.124 seconds			Longitudinal translational mode T= 0.096 seconds		
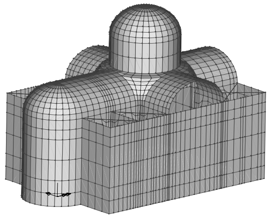	Individual Modal Participating Ratio %			Individual Modal Participating Ratio %		
	Ux	Uy	Uz	Ux	Uy	Uz
	0.00	**54.60**	0.0	**32.41**	0.0	0.071

Model 4 with 3 apses	Transverse translational mode T= 0.115 seconds			Longitudinal translational mode T= 0.106 seconds		
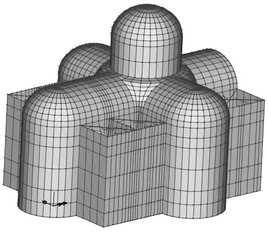	Individual Modal Participating Ratio %			Individual Modal Participating Ratio %		
	Ux	Uy	Uz	Ux	Uy	Uz
	0.00	**53.23**	0.0	**42.73**	0.00	0.011

Table 2: Continued.

Model 5 with 3 apses and openings	Transverse translational mode T= 0.116 seconds			Longitudinal translational mode T= 0.109 seconds		
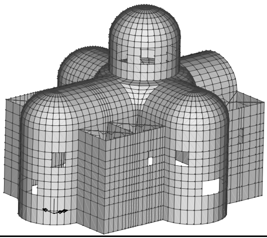	Individual Modal Participating Ratio %			Individual Modal Participating Ratio %		
	Ux	Uy	Uz	Ux	Uy	Uz
	0.00	**55.20**	0.0	**46.27**	0.00	0.015

Model 6 with apses, openings and secondary vaulting	Transverse translational mode T= 0.130 seconds			Longitudinal translational mode T= 0.119 seconds		
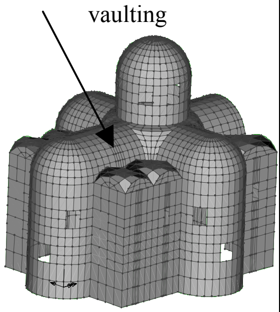	Individual Modal Participating Ratio %			Individual Modal Participating Ratio %		
	Ux	Uy	Uz	Ux	Uy	Uz
	0.0	**51.77**	0.0	**44.76**	0.0	0.07

The sixth model (Model 6 in table 2), which includes the 3 apses the openings of the peripheral walls and central dome together with the secondary vaulting joining the peripheral walls with the central dome, represents a closer resemblance to the real structure from all six numerical simulations of this church. This sixth model was utilized to predict the behaviour of this church under gravitational and earthquake loads.

The inclusion of the 10th mode, for model 6, gives the cumulative modal mass equal to 56.22% of the total mass in the x-x (longitudinal) direction and 60.52% of the total mass in the y-y (transverse) direction. In order to account for the total mass, without the inclusion of eigen-modes further than the 10th, the dynamic analysis results for the earthquake loads in the x-x and y-y directions were amplified by the inverse of the cumulative modal mass participation ratios in the corresponding directions (**fxx = 100/60.52 = 1.652, fyy = 100/56.22 = 1.778)**.

The design spectrum, as defined for old seismic zone III of the Greek seismic code was employed in defining the earthquake loads. The ground design acceleration was taken equal to 0.24g; it was assumed that the local soil conditions belong to soil category B. An importance factor equal to 1.3 was adopted and a load reduction coefficient equal to 1.5 was also assumed (structural elements made of stone masonry).

www.witpress.com, ISSN 1743-3509 (on-line)

The gravitational and earthquake loads were applied simultaneously. The effects of the seismic action in the longitudinal direction are presented in figures 3 and 4 in terms of the areas of failure that are predicted by the two failure criteria that were employed. Figure 3 presents the failure areas (zone 2, zone 3, zone 4) as predicted by the application of the Mohr-Coulomb criterion. These areas are classified in a way that signifies the most predominant state of stress that leads to failure. Similarly, figure 4 presents the corresponding failure areas as predicted by the modified Von-Misses criterion. A similar distinction of these areas as before is also shown. However, in this case the predominant state of stress corresponds to the regions of the employed envelope curve of the adopted failure criterion (figure 2).

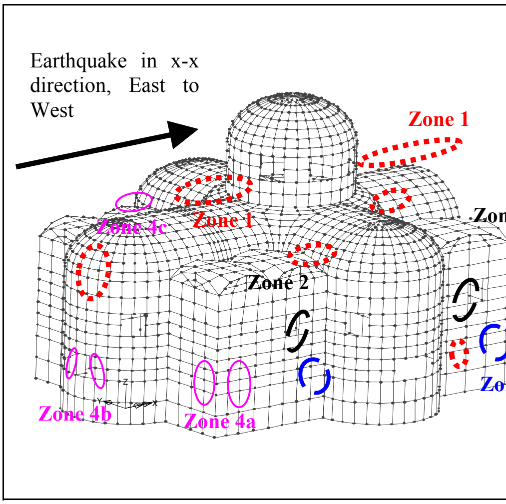

Zone 1: Tensile and Shear stresses are below allowable Tensile and Shear Strengths
Zone 2: Shear stresses are above allowable Shear Strengths
Zone 3: Compressive stresses are above allowable Compressive Strengths
Zone 4: Tensile stresses Are above allowable Tensile Strengths

Figure 3: Comparison of tensile and shear stresses to allowable tensile and shear strengths as predicted by Mohr-Coulomb failure envelope.

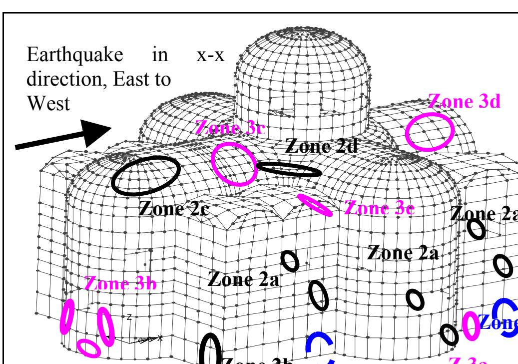

Zone 1: Compression-Compression stress state
Zone 2: Compression-Tension stress state
Zone 3: Tension-Tension stress state

Figure 4: Failure areas as predicted by modified Von Misses failure criterion.

3 Discussion of the results for the Agia Triada church

3.1 Variation of eigen-periods

The influence of the tympana is studied, in the comparison of periods obtained from Model 1 and Model 2. The addition of the tympana resulted in a decrease of 8% and 7% in the corresponding eigen-period values for the two dominant modes.

Comparison of Model 1 and Model 3 show that the translational mode in the longitudinal direction is only marginally affected by the inclusion of the apse. The small percentage of mass participation in this case is possibly a reason behind this observation.

By including apses in both directions as shown in Model 4 the eigen-periods obtained are 6.5% less than that predicted by the Model 1 for the transverse mode, but for the longitudinal mode the eigen-periods predicted by Model 4 are 6.5% higher than those predicted by Model 1.

Comparing Model 4 with Model 3 a noticeable reduction in the eigen-period in the transverse direction can be seen. Whereas, the opposite is true for the eigen-period in the longitudinal direction.

The structure with the openings (Model 5) results, as expected, in higher values of eigen-periods in both directions as compared to the eigen-period values without the openings.

The complete simulation of Agia Triada church is obtained in Model 6.The structure with the secondary vaulting (Model 6) results in higher values of eigen-periods in both directions as compared to the eigen-period values without the secondary vaulting. This is a result of an increase of the total mass of the structure without any significant increase in the stiffness of the structure resulting from the inclusion of the secondary vaulting.

3.2 Failure areas predicted by the application of the two failure criteria

As already stated, the application of two failure criteria have been examined for the church of Agia Triada. Applying the Mohr Coulomb failure criterion the areas where tensile failure is predicted are:

a) At the base of the pier in the east part of the longitudinal peripheral wall (zone 4a figure 3).

b) Below the lower window opening at the apse, which is positioned in the longitudinal direction (zone 4b figure 3).

c) At the crown of the eastern longitudinal main vault near the edge of the apse (zone 4c in figure 3).

Areas where shear failure is predicted, applying the Mohr Coulomb criterion, are the ones where the shear stress values are higher than the ones predicted by equation (1). Such areas exist at the piers of the west and east part of the longitudinal peripheral wall (zone 2 figure 3). At zone 3, the predicted compressive stresses are higher than the assumed compressive strength of masonry. Such areas exist at the base of piers of the west and east part of the longitudinal peripheral wall (zone 3, figure 3). At zone 1, the predicted tensile stresses are less than the assumed tensile strength of masonry. However, these are also areas of potential failure if a lower tensile strength is adopted.

Applying the modified Von-Misses failure criterion areas where tensile failure is predicted are:

a) At the base of the pier in the western part of the longitudinal peripheral wall near the transverse apse (zone 3a figure 4).

b) At the apse which is positioned in the longitudinal direction, below the lower window opening (zone 3b figure 4).

c) At the crown of the east main longitudinal vault near the central dome (zone 3c figure 4).

d) At the crown of the west main longitudinal vault (zone 3d figure 4).

e) At the arches of the main transverse vaulting system (zone 3e figure 4).

Areas where compressive failure is predicted are located at the base of the piers in the longitudinal peripheral wall (zone 1 figure 4).

Areas where combined compressive-tensile failure is predicted are:

a) At the longitudinal peripheral wall in a diagonal direction above and below the window openings (zone 2a figure 4).

b) At the base of the east transverse peripheral wall (zone 2b figure 4).

c) At the crown of the eastern main longitudinal vault near the edge of the apse (zone 2c figure 4).

d) At the base of the central dome (zone 2d figure 4).

4 Conclusions

1) As expected, for the church of Agia Triada the tympana, apses, window openings, and secondary vaulting have a noticeable influence in the stiffness and mass of the structure as was shown by the numerical investigation, which reflects on the values of the predicted fundamental eigen-frequencies.

2) Comparing the failure areas as predicted by the two criteria, a reasonable agreement can be seen for the peripheral walls and apses. However, such types of damage, as the one indicated by these failure criteria, is not clearly observed in the prototype structure.

3) The modified Von-Misses criterion predicts a more widespread failure in the main vaults and at the pendatives near the base of the central dome than the failure predicted by Mohr-Coulomb. This fact is in a better agreement with the observed damage for this church.

References

[1] Manos G.C. et al. “Correlation of the observed earthquake performance of the church of St. Constantine in Kozani-Greece with corresponding numerical predictions”, STREMA97, San Sebastian, Spain, pp. 309-320.

[2] Manos G.C. et al. Earthquake Performance of the Church of St. Constantinos in Kozani-Greece. Correlation of the Observed Damage with Numerical Predictions”, 4th Intern. Symposium on computer methods in Structural Masonry, Sept.1997, Florence, Italy.

[3] G.C. Manos, V. J. Soulis, A. Diagouma, "Preliminary Numerical Investigation of the Dynamic Characteristics of Historical Monuments", 13WCEE, Vancouver, Canada, 2004.
[4] Ghosh K and Amde M "Finite Element Analysis of Infilled Frames", Journal of Structural Engineering, July 2002, pp.881-889.
[5] Proposed Revisions to Eurocode-6 Nov 2002.
[6] Page A.W "The strength of brick masonry under biaxial compression-tension", Int. J. Masonry Constr., 3(1),p 26-31.